

Charge Transfer from Organic Molecules to Molybdenum Disulfide: Influence of the Fluorination of Iron Phthalocyanine

Katharina Greulich,[†] Axel Belser,[†] Sven Bölke,[†] Peter Grüninger,[†] Reimer Karstens,[†] Marie Sophie Sättele,[†] Ruslan Ovsyannikov,[#] Erika Giangrisostomi,[#] Tamara V. Basova,^{||} Darya Klyamer,^{||} Thomas Chassé,^{‡, †} and Heiko Peisert^{†*}

[†] Institute of Physical and Theoretical Chemistry, University of Tübingen, Auf der Morgenstelle 18, 72076 Tübingen, Germany

[#] Institute for Methods and Instrumentation in Synchrotron Radiation Research, Helmholtz-Zentrum Berlin für Materialien und Energie GmbH, Albert-Einstein-Strasse 15, 12489 Berlin, Germany

^{||} Nikolaev Institute of Inorganic Chemistry SB RAS, 3 Lavrentiev Ave., Novosibirsk, Russia 630090

[‡] Center for Light-Matter Interaction, Sensors & Analytics (LISA⁺) at the University of Tübingen, Auf der Morgenstelle 18, 72076 Tübingen, Germany

* Corresponding author, heiko.peisert@uni-tuebingen.de, Tel.: (+49) 07071 / 29-76931, Fax: (+49) 07071 / 29-5490

Abstract

Layered transition metal dichalcogenides (TMDCs), such as molybdenum disulfide (MoS_2), are currently in the focus of interest due to their novel electronic properties. The adsorption of molecules is a promising way to tune the electronic structure of TMDCs. We study interface properties between MoS_2 and differently fluorinated iron phthalocyanines (FePcF_x , $x = 0, 4, 16$) using X-ray photoelectron spectroscopy (XPS), Ultraviolet photoelectron spectroscopy (UPS), angle-resolved photoelectron spectroscopy (ARPES) and X-ray absorption spectroscopy (XAS). A key parameter for the charge transfer is the ionization potential of FePcF_x . A distinct electron transfer from the molecule to the substrate is observed for FePc and FePcF_4 . From energy-momentum ARPES maps we suppose that substrate and FePc related states hybridize at the interface. This study demonstrates that a controlled tuning of the electronic structure of MoS_2 by electron donors is possible, driven by the ionization potential difference between substrate and adsorbate.

1. Introduction

The recently increasing research efforts devoted to layered transition metal dichalcogenides (TMDCs) derives from their novel electronic and magnetic properties. As an example, for MoS₂, the size of the bandgap and its nature (indirect or direct) depends on the number of trilayers.¹ Moreover, even the electronic structure of MoS₂ bulk crystals can show regions of high spin-polarization.² Electronic properties of TMDC surfaces might be tuned by the adsorption of molecules. In particular, this was shown for strong electron acceptors like (fluorinated) tetracyanoquinodimethane (TCNQ) or fluorinated fullerenes.³⁻⁷ The formation of covalent bonds is observed most notably for metallic TMDCs or for TMDC monolayers, where, caused by the preparation conditions, defect sites exist.⁶

Transition metal phthalocyanines (TMPcs) might be especially suited for systematic studies of charge transfer processes because of their chemical tunability of electronic and magnetic properties. Therefore, TMDC/TMPc heterostructures may exhibit novel electronic properties, which could be of high interest for efficient and flexible electronics, photonics and spintronics.^{6,8} Recently, the interface between (transition metal) phthalocyanines and TMDCs has been attracting a lot of attention and charge transfer processes have been studied by various methods, especially with a focus on its use in photodetection.⁹⁻¹⁴ For applications, the charge transfer dynamics of excited states at MoS₂ interfaces is of enormous importance. Ultrafast (hot) electron transfer was recently reported for several MoS₂ interfaces.¹⁵⁻¹⁶ Furthermore, it is worth to mention that MoS₂/FePc hybrid nanostructures exhibit excellent catalytic activity for both the hydrogen evolution reaction and the oxygen reduction reaction.¹⁷ Even if the charge transfer at TMPc interfaces is expected to be bidirectional in many cases,¹⁸⁻²⁰ the charge transfer via the transition metal is a peculiar channel that may change the electronic configuration at the interface. In most cases, the fluorination of TMPcs

changes basic electronic properties like the ionization potential but leaves the electronic structure of the central metal atom unchanged. We expect that this may be different for FePc and FePcF₁₆ based on our recent studies of perfluorinated FePc films on Cu and Ag single crystals.²¹⁻²² In order to shed more light on the interplay between the degree of fluorination, molecular arrangement and electronic configuration, we studied the electronic structure of FePc, FePcF₄ and FePcF₁₆ on MoS₂ as a function of the film thickness.

2. Experimental

Synthetically grown 2H-phase MoS₂ was purchased from 2DSemiconductors Inc., USA and glued to the sample holder by UHV-rated conductive epoxy. To obtain a clean (0001) surface, the crystal was cleaved by adhesive tape in ultrahigh vacuum (UHV). The cleanliness and the azimuthal orientation of the surface were checked by X-ray photoelectron spectroscopy (XPS), ultraviolet photoelectron spectroscopy (UPS) and angle-resolved photoelectron spectroscopy (ARPES). We note that, generally, the preparation of MoS₂ might result in inhomogeneous surface regions, visible, e.g., in a broadening of photoemission features and a splitting of the high binding energy cutoff in UPS. In such cases, a new preparation was performed. The laterally resolved distribution of S 2p_{3/2} binding energies in Figure S1 (supplementary information) demonstrates that large homogeneous regions can be prepared.

For calibration purposes, we used Au and Cu foils (of 99.95% and 99.9% purity, respectively) purchased from Goodfellow Cambridge Ltd, England. The foils were cleaned by repeated cycles of argon ion sputtering.

FePc was purchased from Sigma Aldrich Chemie GmbH, Germany and FePcF₁₆ from Synthon Chemicals & Co KG, Germany. The powders were resublimed for further purification. FePcF₄ was synthesized by heating of a 4:1 mixture of 4-fluorophthalonitrile (Sigma Aldrich Chemie

GmbH) and iron(II) oxalate in a glass tube at 190 °C for 4 hours. The resulting product was purified by gradient sublimation in vacuum ($1.33 \cdot 10^{-5}$ mbar) at 440 °C. FePcF₄ was obtained as a statistical mixture of four regioisomers due to various possible positions of fluorine substituents. No attempt was made to separate them because of the proximity of the sublimation parameters.

The FePcF_x powders were placed in a home-built Knudsen cell and the deposition on the MoS₂ crystal was accomplished by resistively heating the cell to 390 °C. The deposition rates of 0.2-0.3 nm/min were monitored by a quartz microbalance. The nominal layer thickness was estimated from the XPS intensity ratios of substrate and overlayer core level spectra assuming layer by layer growth. Sensitivity factors from Yeh and Lindau were used.²³ The mean free paths were calculated according to Seah and Dench.²⁴

X-Ray absorption spectroscopy (XAS) and ARPES measurements using synchrotron radiation were performed at the LowDosePES endstation of the PM4 beamline (BESSY II, Helmholtz-Zentrum Berlin, Germany).²⁵⁻²⁶ This endstation is equipped with an angle-resolved time-of-flight (ArTOF) analyzer used for both ARPES and XAS measurements. An improved detection efficiency by a factor of roughly two to three orders of magnitude with respect to more conventional hemispherical analyzers allows measurements with very limited photon flux avoiding radiation damage of sensitive organic molecules.²⁵ Polarization-dependent XAS measurements at the N K and Fe L edges were carried out in total electron yield. Different angles of the incident polarized light with respect to the sample surface plane were chosen. The energy resolution for ARPES measurements was 55 meV.

XPS and UPS measurements in the home lab were performed using a multi-chamber UHV system with a base pressure of $2 \cdot 10^{-10}$ mbar, equipped with a monochromated Al-K_α

radiation source (XR 50 M, Specs), an Ultraviolet source (UVS 300 SPECS) and a Phoibos 150 hemispherical photoelectron analyzer. Core level spectra of Au and Cu foils were measured for a calibration of the binding energy scale with respect to the Au 4f_{7/2} (84.0 eV) and the Cu 2p_{3/2} (932.6 eV) peak positions. The energy resolution was 400 meV and 150 meV for XPS and UPS, respectively.

3. Results and Discussion

3.1. Molecular Orientation and Electronic Structure in Thin Films

The detailed arrangement of molecules at interfaces is crucial for interactions between molecule and substrate-related orbitals and thus interface properties can be distinctly affected by the molecular orientation. Therefore, we will first discuss the molecular orientation of FePcF_x molecules in thin films on MoS₂.

XAS (also called near edge X-ray absorption fine structure, NEXAFS) is a valuable tool for the determination of orientation of planar molecules in ultrathin films.²⁷⁻²⁸ For phthalocyanines, besides the commonly used C 1s- π^* also N 1s- π^* excitations are available, which can be used for the analysis of the molecular orientation in a similar manner.²⁹ Intensity arising from N 1s $\rightarrow \pi^*$ transitions becomes maximal if the electric field vector **E** of the incoming synchrotron light is parallel to the p_z orbitals, i.e. perpendicular to the molecular plane. Vice versa, transitions to σ^* states will dominate if **E** is parallel to the molecular plane.

In the upper panels of Figure 1 a), b) and c), we compare N K XAS spectra of FePc, FePcF₄, and FePcF₁₆ on MoS₂ for two prominent angles of incidence. The measurement geometry is depicted in the inset of Figure 1: 20° corresponds to grazing incidence and 90° to normal incidence of the p-polarized synchrotron light with respect to the substrate surface. The shape of the N K XAS spectra is typical for phthalocyanines; features at photon energies lower than

about 402 eV are mainly attributed to $N\ 1s \rightarrow \pi^*$ transitions.²⁹⁻³³ For FePc and FePcF₁₆ an additional feature below 399 eV is recognizable, which is attributed to a Mo M edge absorption. Due to the larger film thickness, this feature is strongly attenuated for FePcF₄.

Clearly visible in Figure 1, all three investigated FePcF_x molecules show a strong dichroism in thin films with thicknesses larger than 4.5 nm. The strongest intensity of $N\ 1s \rightarrow \pi^*$ orbitals at grazing incidence implies that the molecules are predominantly flat lying with respect to the substrate surfaces. The fact that the remaining intensity in the range of π^* transitions is almost negligible at normal incidence indicates small tilt angles and a high degree of ordering in films thicker than 4 nm. We note that indications for the possibility of a preferred flat lying orientation are also observed for lower coverages, however, the analysis of the corresponding XAS spectra is more complicated due to a dominant intensity of the substrate-related Mo M edge in these spectra (see supplementary information, Figure S2).

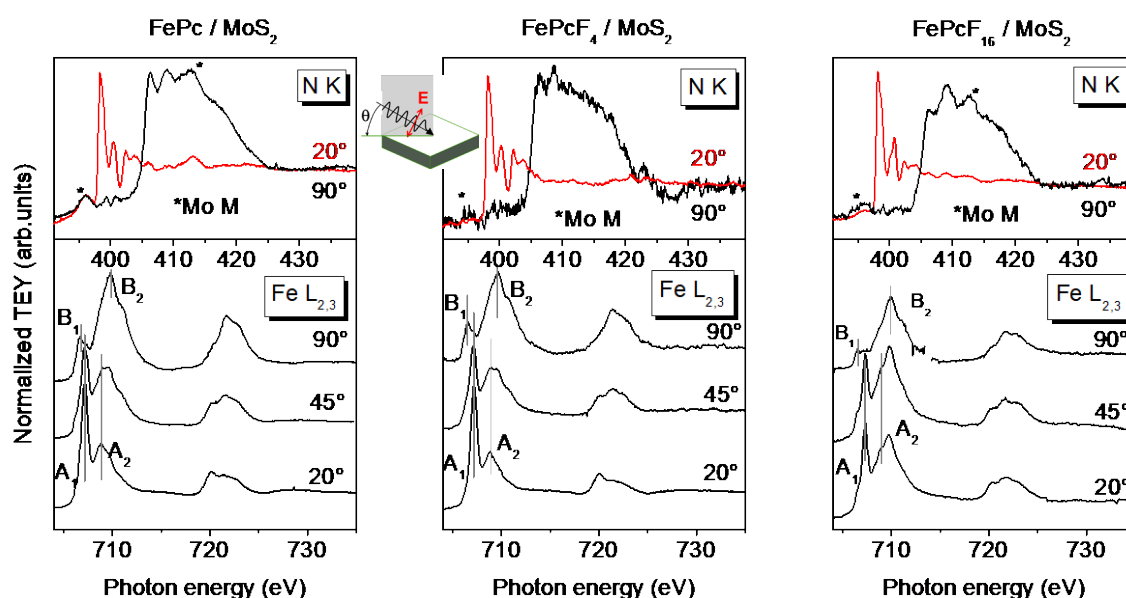


Figure 1. *N K edge (top) Fe L_{2,3} edge (bottom) XAS spectra of FePcF_x films on MoS₂: a) FePc (thickness 4.5 nm), b) FePcF₄ (thickness 7.8 nm) and c) FePcF₁₆ (thickness 5.3 nm). Although *N K edge* spectra indicate almost flat lying molecules in all cases, the overall shape of the*

Fe L_{2,3} edge is rather similar for FePc and FePcF₄, but exhibits few striking differences for FePcF₁₆.

A clear angular dependence is also visible for the Fe L_{2,3} spectra shown in the lower panels of Figure 1. This dichroism is also caused by the orientation of the molecules: For the almost flat lying adsorption geometry, as determined from N K XAS spectra, transitions into orbitals parallel to the molecular plane (e. g. $d_{x^2-y^2}$ and d_{xy} states) are preferentially probed at normal incidence, whereas orbitals with out-of-plane components (e. g. d_{xz} , d_{yz} , d_{z^2} states) exhibit distinct intensity at grazing incidence. At the chosen film thicknesses larger than 4 nm, contributions from the first monolayer and thus possible effects caused by interactions with the substrate are negligible, i.e. bulk-like film properties are probed.

The Fe L_{2,3} spectra in Figure 1 remind strongly of FePc films on single crystalline metal substrates (see, e.g., Refs. ^{30, 33-36}), we will discuss briefly the shape of the L₃ edge (705-715 eV). The spectra recorded at grazing incidence are dominated by an intense peak at 707.1 eV, denoted A₁, whereas the spectra at normal incidence exhibit contributions from a low photon energy feature B₁ at 706.3 eV and a broad feature B₂ centred at about 709 eV. From the angular dependence, considering the almost flat molecular orientation, we conclude that A features arise from transitions into orbitals with out-of-plane contributions (e.g. d_{z^2}), whereas B features are dominated by transitions in the molecular plane (e.g. into $d_{x^2-y^2}$). Since multiplet effects determine the shape of XAS spectra of transition metal L edges to a large extent, the different peaks cannot be assigned to a particular transition without extensive theoretical analysis, possibly also accounting for mixed valences. For a more detailed, partially controversial discussion of the ground state of Fe in FePc and the shape of Fe L edge XAS spectra, we refer to the literature (e.g. Refs. ^{21, 37-42}).

Despite the overall similarity of the Fe L edge XAS spectra of the three phthalocyanines in Figure 1, differences can be identified. Whereas the spectra for FePc and FePcF₄ are almost identical, the relative intensities of A and B features for FePcF₁₆ exhibit several striking differences to the former ones. This is most visible in the spectrum measured at grazing incidence, where the A₁/B₂ ratio is distinctly decreased compared to FePc. Since the molecular orientation is similar for all three phthalocyanines, such changes of the peak shape must be ascribed to a different electronic structure of the central Fe atom in FePcF₁₆ compared to FePc and FePcF₄. We note that an even more pronounced intensity increase of B₂ in Fe L₃ XAS spectra was recently observed for FePcF₁₆ on Ag(111) and Cu(111).²¹ Most likely, the detailed electronic structure depends sensitively on the molecular arrangement in thin films and, possibly, on intermolecular interactions.²¹ Therefore, the different shape of the Fe L edge XAS spectra for FePcF₁₆ on MoS₂ compared to the Ag(111) and Cu(111) surfaces²¹⁻²² may point to a slightly different arrangement of the molecules in the thin films, most likely caused by a weaker interaction at the interface to the van-der-Waals surface of MoS₂ and/or different preparation conditions.

3.2. Interface Properties

Generally, on van-der-Waals surfaces such as MoS₂(0001), a weak physisorption of organic molecules might be expected, accompanied with the absence or a moderate redistribution of electrons at the interface. In contrast, for chemisorbed molecules on more reactive surfaces, a local interaction and the formation of bonds might be observed, visible as interface components in XPS and XAS spectra. We note that we do not observe such interface components for all three investigated phthalocyanines in Fe L edge XAS spectra, C 1s XPS

spectra and Fe 2p XPS spectra (cf. Figures S2 and S3, supplementary information), indicating the absence of local charge transfer (which affects a specific atom only).

On the other hand, in particular for strong electron acceptors, a significant charge transfer was recently reported on bulk or single-layer van-der-Waals surfaces.^{3-5, 7} If the energy levels of the substrate and the overlayer differ distinctly, the prediction of a possible charge transfer is comparatively straightforward. According to the Integer Charge Transfer (ICT) model, a charge transfer at such weakly interacting interfaces becomes possible if the work function of the substrate is larger than the positive polaron (close to the highest occupied molecular orbital, HOMO) or smaller than the negative polaron (close to the lowest unoccupied molecular orbital, LUMO) of the organic semiconductor.⁴³⁻⁴⁴ Thus, for systematic studies, variation of either the substrate work function or of the electronic properties of the organic semiconductor is needed. The fluorination of phthalocyanines provides the opportunity to vary the ionization potential IP of the molecule while leaving other electronic properties such as the composition of HOMO and LUMO or the optical gap almost unaffected.⁴⁵⁻⁴⁸

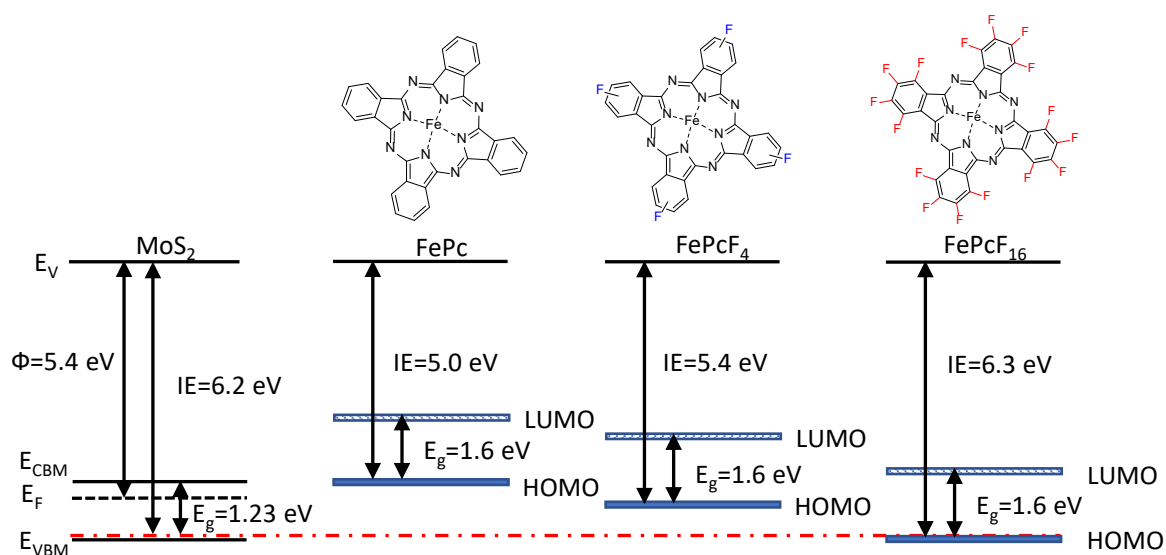


Figure 2. Comparison of the position of important energy levels of FePcF_x with respect to the MoS₂ substrate as obtained from UPS. Energy gaps (E_g) were determined by UV-VIS (FePcF_x) or taken from the literature (MoS₂, Ref.⁴⁹). All individual diagrams are aligned at the respective vacuum energies.

In Figure 2, we compare the positions of important electronic levels of FePcF_x in thin films with respect to the MoS₂ substrate as obtained from UPS. The corresponding spectra are shown in Figure S4 (supplementary information). The work function Φ and the HOMO onset (valence band maximum, VBM) were determined by linear extrapolation of the secondary electron cutoff and the raising edge of the HOMO peak, respectively. IE corresponds to the sum of Φ and E(HOMO). The reference in Figure 2 is the vacuum level (E_v) for all materials. As energy gap (E_g) of FePcF_x we used the optical gap, determined by UV-VIS (see Figure S5, supplementary information), E_g of MoS₂ was taken from the literature.⁴⁹

The valence band spectrum of the clean MoS₂ substrate is in excellent agreement with the literature⁵⁰⁻⁵¹ and can be reproduced very well for different samples. The measured Φ (5.4 eV) and VBM (0.8 eV) of MoS₂ implies that the substrate is slightly n-doped, considering the band gap of 1.23 eV.⁴⁹

As can be seen from Figure 2, the HOMO position of the three phthalocyanines is distinctly different with respect to the substrate-related energy levels VBM and CBM (conduction band minimum). Only for FePc and FePcF₄ the HOMO is located above the VBM of MoS₂, and even at or above the Fermi level position, which might enable an electron transfer from the molecule into substrate related gap states. Assuming an exciton binding energy of 0.5-0.6 eV as observed for many organic semiconductors,⁵²⁻⁵³ the positive polaron is expected distinctly above the CBM of MoS₂ for FePc and close to CBM for FePcF₄, enabling an integer charge transfer from the molecule to the conduction band of the substrate. In contrast, due to the higher ionization potential, FePcF₁₆ could rather act as an electron acceptor. However, the

LUMO position and the negative polaron energy (assuming an exciton binding energy of 0.6 eV) does not exceed the high ionization potential of MoS₂ and, therefore absence of a charge transfer is expected at the FePcF₁₆/MoS₂ interface.

A distinct charge transfer between the molecules and the substrate would be accompanied by formation of an interface dipole. We note, however, that also other reasons might contribute to dipoles, as was intensely discussed in the literature (e.g Refs.⁵⁴⁻⁵⁷). The formation of interface dipoles can be monitored by a shift of the work function upon deposition of the molecule.

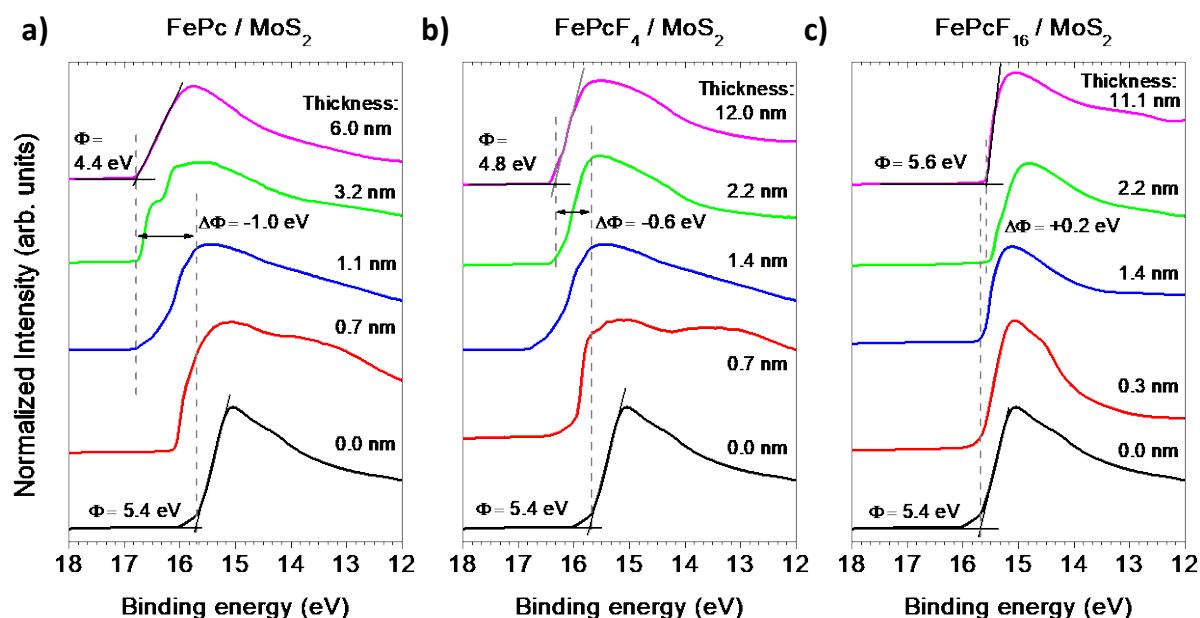


Figure 3. Enlarged section of the secondary electron cutoff region of He-I UPS spectra for different FePcF_x/MoS₂ interfaces as a function of the film thickness: a) FePc/MoS₂ b) FePcF₄/MoS₂ c) FePcF₁₆/MoS₂.

An enlarged section of the secondary electron cutoff (SECO) region of the UPS valence band spectra (HeI, $h\nu = 21.22$ eV) is shown in Figure 3 for different coverages of FePcF_x on MoS₂.

Complete energy level alignment diagrams are shown in Figure 4. The work function Φ of the

sample was calculated according to $\Phi = 21.22 \text{ eV} - E(\text{SECO})$. A change of the cutoff-position indicates directly the formation of an interface dipole. Significant changes in the cutoff positions in Figure 3 are noticeable for increasing film thicknesses of FePc and FePcF₄ on MoS₂, whereas for FePcF₁₆ on MoS₂ Φ is hardly influenced by the thickness. In this manner, the Fermi level of the substrate aligns with a midgap position of the FePcF₁₆ HOMO-LUMO gap. Notably, this position is almost the same for all the three Pc molecules considered here.

There are many possible reasons for small Φ changes as observed for FePcF₁₆/MoS₂ (0.2 eV). For instance, thickness-dependent changes of the ionization potential (e.g. due to a change of the molecular arrangement), a change of the work function of the substrate upon adsorption or a weak redistribution of electrons at the interface may occur (see, e.g. Refs. ⁵⁸⁻⁶⁰). Thus, small interface dipoles do not necessarily imply the occurrence of a charge transfer across the interface. On the other hand, stronger shifts of $E(\text{SECO})$ in Figure 3 are observed upon adsorption of FePc and FePcF₄, corresponding to a decrease of the work function by 1.0 eV and 0.6 eV, respectively. We note that an initial reduction of Φ can be ascribed to the push back or pillow effect (where surface electron density is pushed back into the substrate by Pauli repulsion of the adsorbate's electron density), whose size on organic/metal interfaces is often in the order of 0.3 eV.^{55, 61-63} However, for interfaces controlled by van-der-Waals forces, we expect that this effect contributes less to the interface dipole. Therefore, the appearance of interface dipoles as high as -0.6 and -1.0 eV might be a first indication for a charge transfer from the FePc and FePcF₄ molecules to the MoS₂ substrate and rather likely related to the midgap Fermi level positions in the molecular semiconductor films.

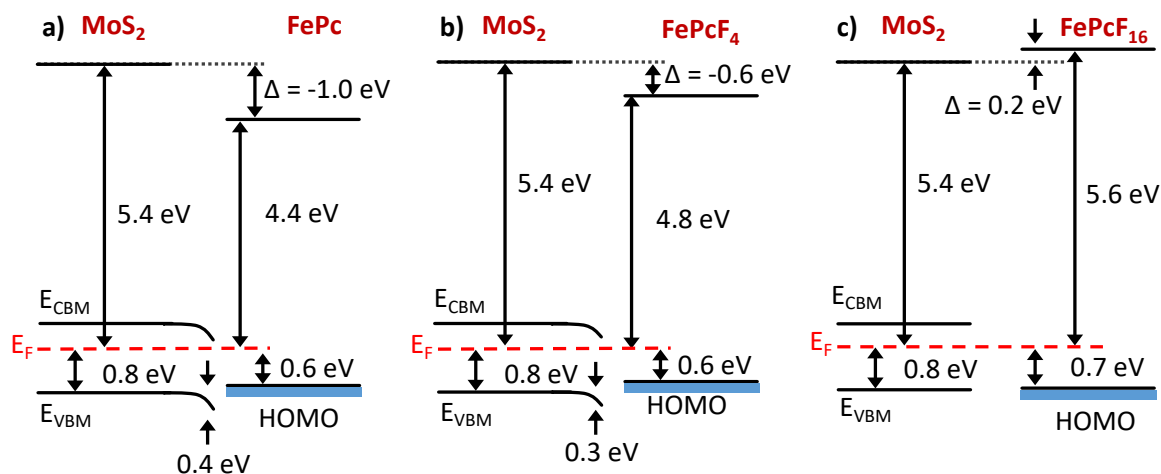


Figure 4. Energy level diagrams of Fe phthalocyanines with a different degree of fluorination: a) FePc/MoS₂, b) FePcF₄/MoS₂ and c) FePcF₁₆/MoS₂.

The occurrence of different dipoles at the three investigated interfaces is summarized in the diagrams of Figure 4, depicting the energy level alignment for FePcF_x the thickest films with a film thickness between 6 and 12 nm. The situation for 2-3 nm thick films would be comparable to the film thicknesses used here (cf. Figure 3). Note that the E_v position in Figure 4 for the uncovered substrate may change because of band bending at the interface, discussed below in detail.

Also visible in Figure 4, the relative positions of the HOMO with respect to the Fermi level E_F or VBM of the substrate are surprisingly similar for all investigated phthalocyanines (0.6-0.7 eV below E_F). In the frame of the ICT model this would mean that the positive polaron level of FePc and FePcF₄ is located 0.6-0.7 eV above the HOMO, a value which is not unlikely (see above). In the case of FePcF₁₆, almost no interaction is expected, and vacuum level alignment occurs, resulting coincidentally in an E_F-HOMO separation of 0.7 eV. We note that different models may explain the observed energy level alignment. A HOMO position distinctly below E_F is observed in models, where the density of gap states of the organic

semiconductor controls the energy level alignment (see, e.g. Refs. ^{57,64}). Thus, if this is similar for all three phthalocyanines, a similar HOMO position with respect to the energy levels of the substrate might be expected. On the other hand, interface states might be formed or modified as a result of the adsorption of molecules (see below).

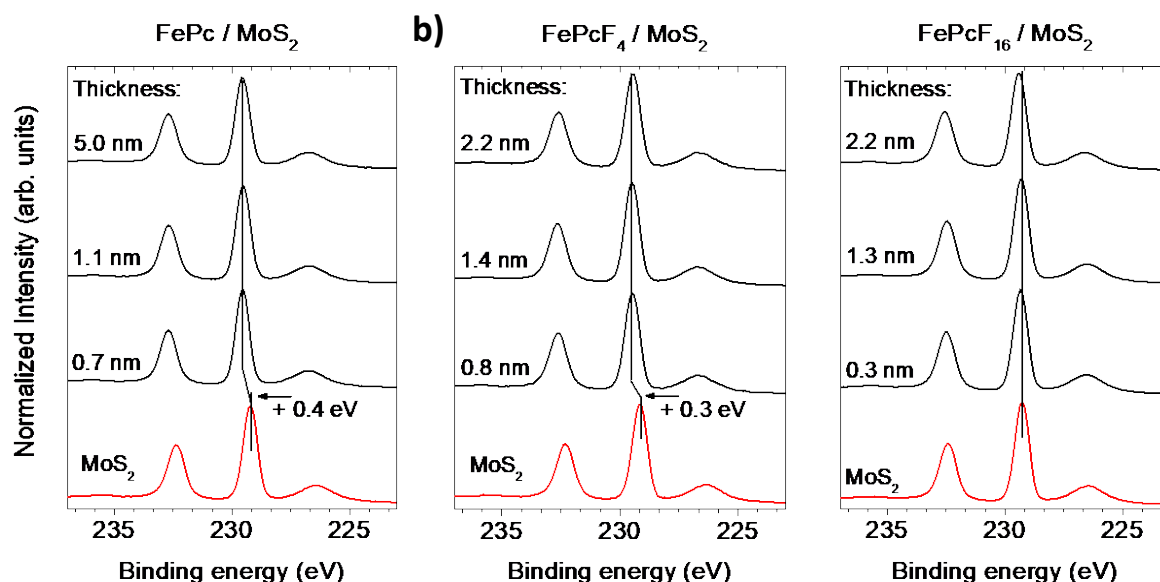


Figure 5. Mo 3d core level spectra as a function of the overlayer thickness: a) FePc/MoS₂, b) FePcF₄/MoS₂ and c) FePcF₁₆/MoS₂.

An interfacial charge transfer to a semiconductor such as MoS₂ would result in an interfacial doping, which might be visible as a shift of the (surface) Fermi level. Since the reference level in photoemission is E_F , this would induce rigid shifts of all valence and core levels. Because core level spectra are usually narrower and not overlapped by adsorbate related features, they are well suited to monitor such surface band bending effects.

In Figure 5, we show substrate-related Mo 3d core level spectra as a function of the FePcF_x overlayer thickness. Only for FePc and FePcF₄, energetic shifts to higher binding energy are visible upon adsorption of the molecules, indicating a band bending at the substrate surface by adsorption-induced n-doping at the interface. The substrate-related S 2p core level spectra

show the same trend (cf. Figure S6, supplementary information). This is a further hint for an electron transfer from the FePc and FePcF₄ molecules to the MoS₂ substrate. On the other hand, the absence of shifts of the binding energy of Mo 3d for FePcF₁₆/MoS₂ hints at the absence of an interfacial charge transfer and a rather inert interface. We note that band bending was observed for other heterojunctions between inorganic and organic semiconductors, depending on the relative electron affinities and ionization energies of the solids.⁶⁵ The trend in the size of band bending for FePc/MoS₂ (0.4 eV), FePcF₄/MoS₂ (0.3 eV) FePcF₁₆/MoS₂ (0.0 eV) follows the differences of the ionization energies between the substrate and the organic semiconductors as extracted from Figure 2 (-1.2, -0.8 and 0.1 eV for FePc/MoS₂, FePcF₄/MoS₂ and FePcF₁₆/MoS₂, respectively).

More information about charge transfer might be extracted from a closer inspection of the lowest energy features in valence band spectra. In Figure 6, we discuss valence band spectra taken at 75 eV excitation energy, integrated over angles of $\pm 15^\circ$ with respect to the surface normal. These experimental parameters correspond to an integration in the k-space region of $k_{||} = \pm 1.2 \text{ \AA}^{-1}$, which includes the K and M points of the MoS₂ substrate, in particular if the Γ point is not exactly centered (see Figure S7, supplementary information). The mapping of different k-space regions compared to measurements using He I excitation (cf. Figure 3 and S4) causes a different spectral weight of valence band features including features close VBM (only features close to the Γ point are mapped in experiments using He I excitation). The error of absolute binding energies in Figures 6 and 7 is estimated to be about ± 0.1 eV.

The top spectra in the upper panels show typical valence band spectra of the three phthalocyanines, the bottom spectra are related to the clean substrate. The slightly different relative intensity of valence band features is most likely due to minor differences in the sampled angular ranges. The intermediate film thickness of 0.3-0.8 nm corresponds to a

coverage in the range of 1-2 monolayers of flat lying molecules, containing contributions from the interface. The 1-2 monolayer spectra for both FePc and FePcF₄ on MoS₂, exhibit a peak at about 1 eV binding energy which has a distinctly different shape than the HOMO in the thin film, whereas for FePcF₁₆ only a small shoulder located close to the MoS₂ valence band maximum is noticeable. This is best visible in the lower panels of Figure 6, where we zoom into the low binding energy region and compare these spectra to the clean substrate. The low binding energy peaks of FePc and FePcF₄ are composed of several components; the shape is clearly different to the HOMO in thicker films. Many reasons may explain a different peak shape depending on the film thickness, including interactions with the substrate or intermolecular interactions.⁶⁶⁻⁶⁷

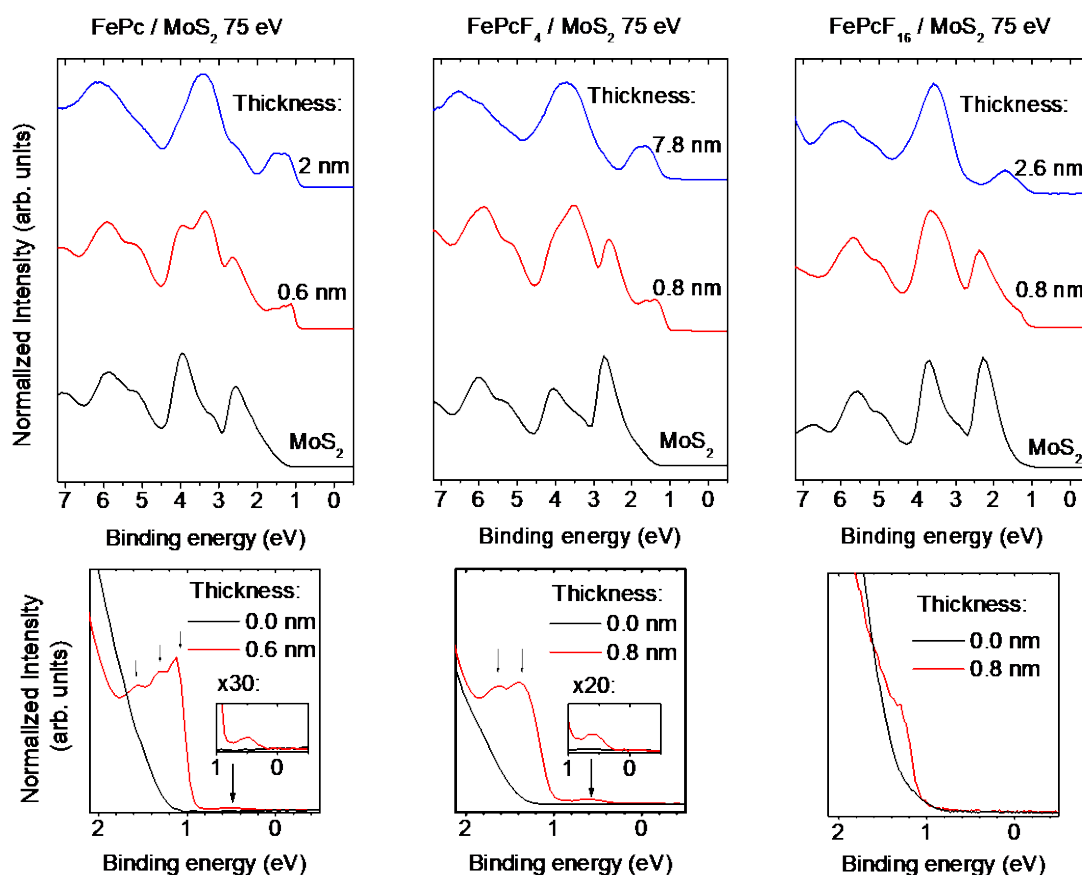


Figure 6. Integrated UPS valence band spectra taken at 75 eV ($k_{||} = \pm 1.2 \text{ \AA}^{-1}$). a) FePc/MoS₂, b) FePcF₄/MoS₂ and c) FePcF₁₆/MoS₂. In the figures in the bottom, the spectra region close to the Fermi energy is enlarged.

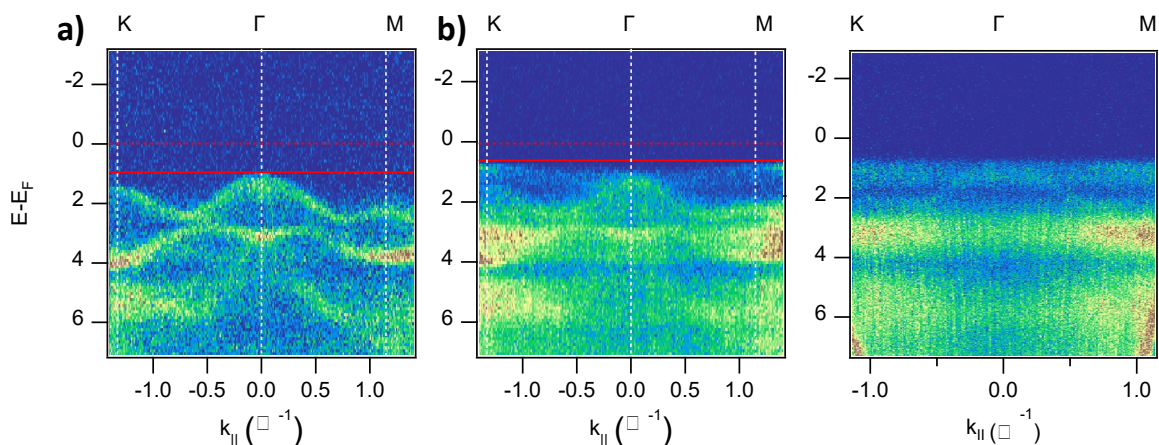
In addition, for FePc/MoS₂ and FePcF₄/MoS₂ weak additional intensity in the gap is recognized in Figure 6 (around 0.5 eV), pointing to the formation of interface states. These interface states might be ascribed to localized states arising from local Mo d-orbital electrons accumulated near a defect site, as theoretically predicted for related phthalocyanines (CuPc and TiOPc) on monolayer MoS₂.⁸ For related Fe-porphyrin / MoS₂ interfaces, the appearance Fe-Mo hybrid states was reported.⁶⁸ We note that also for other molecules surface-confined electronic interactions between adsorbed molecules and localized TMDC (SnS₂) gap states were observed.⁶⁹⁻⁷⁰

In order to analyze the nature of the feature at around 1 eV binding energy in more detail, we discuss energy-momentum ARPES intensity maps using the example of FePc in Figure 7 (excitation energy 75 eV). The x-axis was calibrated using k_x - k_y momentum maps, as described in Figure S7 (supplementary information). The ARPES band map of the clean MoS₂ substrate in Figure 7 a) is in good agreement with the literature.⁷¹ The band with the lowest binding energy is mostly derived from a hybridization of Mo 4d and S 3p orbitals and has maxima at the Γ and K points.⁷¹⁻⁷³ In the ARPES band map of MoS₂ covered with 0.6 nm FePc (Figure 7 b), substrate-related bands are significantly attenuated. Additional intensity after adsorption of FePc is clearly visible at higher binding energies (> 3 eV), but also around 1 eV. Remarkably, the intensity around 1 eV binding energy is inhomogeneously distributed with intensity maxima at emission angles apparently close to the Γ and M points. We note that for highly ordered, periodic structures like acenes, strong intensity variations in the k-space might appear, caused by the orbital distribution in real space.⁷⁴⁻⁷⁵ Indeed, an intensity variation with

the angle of emitted electrons is also observed for phthalocyanines, a maximal intensity is observed around $1.5\text{-}1.7 \text{ \AA}^{-1}$.^{14, 66, 76} However, mainly due to the different distribution and symmetry of molecular orbitals, the intensity variation is much less pronounced compared to acenes. Indeed, in contrast to the monolayer coverage, we do not observe strong intensity variations in range $k_{||} = \pm 1.4 \text{ \AA}^{-1}$ for the highly oriented, almost flat lying FePc molecules in the 2 nm thick film on MoS₂ – a film thickness, where substrate and interface related features are almost vanished (Figure S8, supplementary information).

Also, a slight dispersion of the lowest binding energy feature at around 1 eV is noticeable in Figure 7 b), which is not visible in the energy-momentum map for the 2 nm thick FePc film in Figure 7 c). Since an intermolecular band dispersion, usually only observed in the π -stacking direction of aromatic molecules (cf., e.g., Ref. ⁶⁶), can be excluded for the low coverage of flat lying FePc molecules on MoS₂ in $k_{||}$ direction, a possible origin might be a substrate mediated band dispersion as observed for other π -conjugated molecules on Ag(110).⁷⁷ It was reported that hybridization between molecular and substrate states can substantially increase the delocalization of the molecular states in selective directions along the surface.⁷⁷

Therefore, we suppose that in Figure 7 b) not only molecule related states (i.e. the HOMO) contribute to the feature at lowest binding energy. Rather, we suggest that MoS₂ and FePc-related states hybridize at the interface.



4. Figure 7. Energy-momentum ARPES intensity maps ($h\nu = 75$ eV) of a) clean MoS_2 , b) 0.6 nm FePc on MoS_2 and c) 2.0 nm FePc on MoS_2 . The intensity of the lowest binding energy feature for FePc on MoS_2 is inhomogeneously distributed with intensity maxima close to K and M , pointing to the formation of an hybrid state involving substrate and adsorbate states. **Summary**

The molecular orientation of differently fluorinated iron phthalocyanines (FePcF_x , $x = 0, 4, 16$) on MoS_2 in thin films is very similar. In principle, the almost flat lying adsorption geometry in all three cases allows a comparable interaction between substrate and molecule related orbitals. However, despite the similar orientation, the interaction at the interface is different, depending on the ionization potential difference between substrate and adsorbate. A charge transfer from the molecule to the MoS_2 substrate is observed for the molecules with the lowest ionization potential (FePc and FePcF_4), whereas the $\text{FePcF}_{16}/\text{MoS}_2$ interface is relatively inert. The charge transfer causes a large interface dipole, the formation of interface (gap) states and a band bending in the MoS_2 substrate. From energy-momentum ARPES maps we suppose that MoS_2 and FePc related states hybridize at the interface.

Supporting Information

XY-map of S $2p_{3/2}$ core level binding energy on MoS_2 sample, N K and Fe L XAS of lower coverage FePcF_x layers on MoS_2 , C 1s core level spectra of FePcF_x on MoS_2 , valence band

spectra of FePcF_x on MoS₂ taken with He-I radiation ($h\nu = 21.2$ eV), optical spectra band gap FePc and FePcF₁₆, S 2p core level spectra of FePcF_x on MoS₂ as a function of the overlayer thickness, k_y vs k_x map ($h\nu = 75$ eV) of the clean MoS₂ substrate, energy-momentum ARPES intensity maps ($h\nu = 75$ eV) of 2.0 nm FePc on MoS₂

Acknowledgments

The authors thank the Helmholtz-Zentrum Berlin (HZB) for the allocation of synchrotron radiation. Financial travel support by HZB is thankfully acknowledged. The authors thank Hilmar Adler for fruitful discussions and technical support.

References

1. Wang, Q. H.; Kalantar-Zadeh, K.; Kis, A.; Coleman, J. N.; Strano, M. S., Electronics and Optoelectronics of Two-Dimensional Transition Metal Dichalcogenides, *Nat. Nanotechnol.* **2012**, *7*, 699-712.
2. Gehlmann, M.; Aguilera, I.; Bihlmayer, G.; Mlynczak, E.; Eschbach, M.; Doring, S.; Gospodaric, P.; Cramm, S.; Kardynal, B.; Plucinski, L.; et al., Quasi 2D Electronic States with High Spin-Polarization in Centrosymmetric MoS₂ Bulk Crystals, *Sci. Rep.* **2016**, *6*.
3. Nevola, D.; Hoffman, B. C.; Bataller, A.; Ade, H.; Gundogdu, K.; Dougherty, D. B., Rigid Valence Band Shift Due to Molecular Surface Counter-Doping of MoS₂, *Surf. Sci.* **2019**, *679*, 254-258.
4. Jing, Y.; Tan, X.; Zhou, Z.; Shen, P. W., Tuning Electronic and Optical Properties of MoS₂ Monolayer Via Molecular Charge Transfer, *J. Mater. Chem. A* **2014**, *2*, 16892-16897.
5. Park, S.; Schultz, T.; Xu, X. M.; Wegner, B.; Aljarb, A.; Han, A.; Li, L. J.; Tung, V. C.; Amsalem, P.; Koch, N., Demonstration of the Key Substrate-Dependent Charge Transfer Mechanisms between Monolayer MoS₂ and Molecular Dopants, *Commun. Phys.* **2019**, *2*, 8.
6. Huang, Y. L.; Zheng, Y. J.; Song, Z. B.; Chi, D. Z.; Wee, A. T. S.; Quek, S. Y., The Organic-2D Transition Metal Dichalcogenide Heterointerface, *Chem. Soc. Rev.* **2018**, *47*, 3241-3264.
7. Wang, J. W.; Ji, Z. Y.; Yang, G. H.; Chuai, X. C.; Liu, F. J.; Zhou, Z.; Lu, C. Y.; Wei, W.; Shi, X. W.; Niu, J. B.; et al., Charge Transfer within the F₄TCNQ-MoS₂ van der Waals Interface: Toward Electrical Properties Tuning and Gas Sensing Application, *Adv. Funct. Mater.* **2018**, *28*, 8.
8. Choudhury, P.; Ravavarapu, L.; Dekle, R.; Chowdhury, S., Modulating Electronic and Optical Properties of Monolayer MoS₂ Using Nonbonded Phthalocyanine Molecules, *J. Phys. Chem. C* **2017**, *121*, 2959-2967.
9. Mutz, N.; Park, S.; Schultz, T.; Sadofev, S.; Dagleish, S.; Reissig, L.; Koch, N.; List-Kratochvil, E. J. W.; Blumstengel, S., Excited-State Charge Transfer Enabling MoS₂/Phthalocyanine Photodetectors with Extended Spectral Sensitivity, *J Phys Chem C* **2020**, *124*, 2837-2843.
10. Padgaonkar, S.; Amsterdam, S. H.; Bergeron, H.; Su, K.; Marks, T. J.; Hersam, M. C.; Weiss, E. A., Molecular-Orientation-Dependent Interfacial Charge Transfer in Phthalocyanine/MoS₂ Mixed-Dimensional Heterojunctions, *J Phys Chem C* **2019**, *123*, 13337-13343.

11. Huang, Y.; Zhuge, F.; Hou, J.; Lv, L.; Luo, P.; Zhou, N.; Gan, L.; Zhai, T., Van Der Waals Coupled Organic Molecules with Monolayer MoS₂ for Fast Response Photodetectors with Gate-Tunable Responsivity, *ACS Nano* **2018**, *12*, 4062-4073.
12. Kafle, T. R.; Kattel, B.; Lane, S. D.; Wang, T.; Zhao, H.; Chan, W.-L., Charge Transfer Exciton and Spin Flipping at Organic–Transition-Metal Dichalcogenide Interfaces, *ACS Nano* **2017**, *11*, 10184-10192.
13. Choi, J.; Zhang, H.; Choi, J. H., Modulating Optoelectronic Properties of Two-Dimensional Transition Metal Dichalcogenide Semiconductors by Photoinduced Charge Transfer, *ACS Nano* **2016**, *10*, 1671-1680.
14. Schönauer, K.; Weiss, S.; Feyer, V.; Lüftner, D.; Stadtmüller, B.; Schwarz, D.; Sueyoshi, T.; Kumpf, C.; Puschnig, P.; Ramsey, M. G.; et al., Charge Transfer and Symmetry Reduction at the CuPc/Ag(110) Interface Studied by Photoemission Tomography, *Phys. Rev. B: Condens. Matter* **2016**, *94*, 205144.
15. Shan, H.; Yu, Y.; Wang, X.; Luo, Y.; Zu, S.; Du, B.; Han, T.; Li, B.; Li, Y.; Wu, J.; et al., Direct Observation of Ultrafast Plasmonic Hot Electron Transfer in the Strong Coupling Regime, *Light Sci. Appl.* **2019**, *8*, 9.
16. Johansson, F. O. L.; Cappel, U. B.; Fondell, M.; Han, Y.; Gorgoi, M.; Leifer, K.; Lindblad, A., Tailoring Ultra-Fast Charge Transfer in MoS₂, *Phys. Chem. Chem. Phys.* **2020**, *22*, 10335-10342.
17. Kwon, I. S.; Kwak, I. H.; Kim, J. Y.; Abbas, H. G.; Debela, T. T.; Seo, J.; Cho, M. K.; Ahn, J.-P.; Park, J.; Kang, H. S., Two-Dimensional MoS₂/Fe-Phthalocyanine Hybrid Nanostructures as Excellent Electrocatalysts for Hydrogen Evolution and Oxygen Reduction Reactions, *Nanoscale* **2019**, *11*, 14266-14275.
18. Petraki, F.; Peisert, H.; Uihlein, J.; Aygül, U.; Chassé, T., CoPc and CoPcF₁₆ on Gold: Site-Specific Charge-Transfer Processes, *Beilstein J. Nanotechnol.* **2014**, *5*, 524-531.
19. Lindner, S.; Treske, U.; Knupfer, M., The Complex Nature of Phthalocyanine/Gold Interfaces, *Appl. Surf. Sci.* **2013**, *267*, 62-65.
20. Huang, Y.; Wruss, E.; Egger, D.; Kera, S.; Ueno, N.; Saidi, W.; Bucko, T.; Wee, A.; Zojer, E., Understanding the Adsorption of CuPc and ZnPc on Noble Metal Surfaces by Combining Quantum-Mechanical Modelling and Photoelectron Spectroscopy, *Molecules* **2014**, *19*, 2969-2992.
21. Belser, A.; Karstens, R.; Grüninger, P.; Nagel, P.; Merz, M.; Schuppler, S.; Suturina, E. A.; Chassé, A.; Chassé, T.; Peisert, H., Spin State in Perfluorinated FePc Films on Cu(111) and Ag(111) in Dependence on Film Thickness, *J. Phys. Chem. C* **2018**, *122*, 15390-15394.
22. Belser, A.; Karstens, R.; Nagel, P.; Merz, M.; Schuppler, S.; Chassé, T.; Peisert, H., Interaction Channels between Perfluorinated Iron Phthalocyanine and Cu(111), *Phys. Status Solidi B* **2019**, *256*, 1800292.
23. Yeh, J. J.; Lindau, I., Atomic Subshell Photoionization Cross Sections and Asymmetry Parameters: $1 \leq Z \leq 103$, *At. Data Nucl. Data Tables* **1985**, *32*, 1-155.
24. Seah, M. P.; Dench, W. A., Quantitative Electron Spectroscopy of Surfaces: A Standard Data Base for Electron Inelastic Mean Free Paths in Solids, *Surf. Interface Anal.* **1979**, *1*, 2-11.
25. Giangrisostomi, E.; Ovsyannikov, R.; Sorgenfrei, F.; Zhang, T.; Lindblad, A.; Sassa, Y.; Cappel, U. B.; Leitner, T.; Mitzner, R.; Svensson, S.; et al., Low Dose Photoelectron Spectroscopy at BESSY II: Electronic Structure of Matter in Its Native State, *J. Electron. Spectrosc. Relat. Phenom.* **2018**, *224*, 68-78.
26. Vollmer, A.; Ovsyannikov, R.; Gorgoi, M.; Krause, S.; Oehzelt, M.; Lindblad, A.; Martensson, N.; Svensson, S.; Karlsson, P.; Lundvuist, M.; et al., Two Dimensional Band Structure Mapping of Organic Single Crystals Using the New Generation Electron Energy Analyzer ARTOF, *J. Electron. Spectrosc. Relat. Phenom.* **2012**, *185*, 55-60.
27. Stöhr, J., *NEXAFS Spectroscopy*; Springer; 1992.
28. Stöhr, J.; Outka, D. A., Determination of Molecular Orientations on Surfaces from the Angular Dependence of Near-Edge X-Ray Absorption Fine-Structure Spectra, *Phys. Rev. B: Condens. Matter* **1987**, *36*, 7891-7905.

29. Peisert, H.; Biswas, I.; Knupfer, M.; Chasse, T., Orientation and Electronic Properties of Phthalocyanines on Polycrystalline Substrates, *Phys. Status Solidi B* **2009**, *246*, 1529-1545.
30. Peisert, H.; Uihlein, J.; Petraki, F.; Chassé, T., Charge Transfer between Transition Metal Phthalocyanines and Metal Substrates: The Role of the Transition Metal, *J. Electron. Spectrosc. Relat. Phenom.* **2015**, *204*, 49-60.
31. Willey, T. M.; Bagge-Hansen, M.; Lee, J. R.; Call, R.; Landt, L.; van Buuren, T.; Colesniuc, C.; Monton, C.; Valmianski, I.; Schuller, I. K., Electronic Structure Differences between H₂⁻, Fe⁻, Co⁻, and Cu-Phthalocyanine Highly Oriented Thin Films Observed Using NEXAFS Spectroscopy, *J. Chem. Phys.* **2013**, *139*, 034701.
32. Karstens, R.; Glaser, M.; Belser, A.; Balle, D.; Polek, M.; Ovsyannikov, R.; Giangrisostomi, E.; Chassé, T.; Peisert, H., FePc and FePcF₁₆ on Rutile TiO₂(110) and (100): Influence of the Substrate Preparation on the Interaction Strength, *Molecules* **2019**, *24*, 4579.
33. Betti, M. G.; Gargiani, P.; Frisenda, R.; Biagi, R.; Cossaro, A.; Verdini, A.; Floreano, L.; Mariani, C., Localized and Dispersive Electronic States at Ordered FePc and CoPc Chains on Au(110), *J. Phys. Chem. C* **2010**, *114*, 21638-21644.
34. Petraki, F.; Peisert, H.; Aygul, U.; Latteyer, F.; Uihlein, J.; Vollmer, A.; Chassé, T., Electronic Structure of FePc and Interface Properties on Ag(111) and Au(100), *J. Phys. Chem. C* **2012**, *116*, 11110-11116.
35. Annese, E.; Di Santo, G.; Choueikani, F.; Otero, E.; Ohresser, P., Formation of a Metallic Ferromagnetic Thin Film on Top of an FePc-Ordered Thin Film: The Chemical and Magnetic Properties of the Interface, *J. Phys. Chem. C* **2019**, *123*, 17521-17529.
36. Kroll, T.; Kraus, R.; Schonfelder, R.; Aristov, V. Y.; Molodtsova, O. V.; Hoffmann, P.; Knupfer, M., Transition Metal Phthalocyanines: Insight into the Electronic Structure from Soft X-Ray Spectroscopy, *J. Chem. Phys.* **2012**, *137*, 054306.
37. Stepanow, S.; Miedema, P. S.; Mugarza, A.; Ceballos, G.; Moras, P.; Cezar, J. C.; Carbone, C.; de Groot, F. M. F.; Gambardella, P., Mixed-Valence Behavior and Strong Correlation Effects of Metal Phthalocyanines Adsorbed on Metals, *Phys. Rev. B: Condens. Matter* **2011**, *83*, 220401.
38. Miedema, P. S.; Stepanow, S.; Gambardella, P.; de Groot, F. M. F., 2p X-Ray Absorption of Iron-Phthalocyanine. In *14th International Conference on X-Ray Absorption Fine Structure*, DiCicco, A.; Filipponi, A., Eds. Iop Publishing Ltd: Bristol, 2009; Vol. 190.
39. Miedema, P. S.; de Groot, F. M. F., The Iron L Edges: Fe 2p X-Ray Absorption and Electron Energy Loss Spectroscopy, *J. Electron. Spectrosc. Relat. Phenom.* **2013**, *187*, 32-48.
40. Kuz'min, M. D.; Savoyant, A.; Hayn, R., Ligand Field Parameters and the Ground State of Fe(II) Phthalocyanine, *J. Chem. Phys.* **2013**, *138*, 244308.
41. Kuz'min, M. D.; Hayn, R.; Oison, V., Ab Initio Calculated XANES and XMCD Spectra of Fe(II) Phthalocyanine, *Phys. Rev. B: Condens. Matter* **2009**, *79*, 024413.
42. Stepanow, S.; Lodi Rizzini, A.; Krull, C.; Kavich, J.; Cezar, J. C.; Yakhou-Harris, F.; Sheverdyeva, P. M.; Moras, P.; Carbone, C.; Ceballos, G.; et al., Spin Tuning of Electron-Doped Metal-Phthalocyanine Layers, *J. Am. Chem. Soc.* **2014**, *136*, 5451-5459.
43. Braun, S.; Salaneck, W. R.; Fahlman, M., Energy-Level Alignment at Organic/Metal and Organic/Organic Interfaces, *Adv. Mater.* **2009**, *21*, 1450-1472.
44. Hwang, J.; Wan, A.; Kahn, A., Energetics of Metal-Organic Interfaces: New Experiments and Assessment of the Field, *Mater. Sci. Eng., R* **2009**, *64*, 1-31.
45. Peisert, H.; Knupfer, M.; Schwieger, T.; Fuentes, G. G.; Olligs, D.; Fink, J.; Schmidt, T., Fluorination of Copper Phthalocyanines: Electronic Structure and Interface Properties, *J. Appl. Phys.* **2003**, *93*, 9683-9692.
46. Brinkmann, H.; Kelting, C.; Makarov, S.; Tsaryova, O.; Schnurpfeil, G.; Wohrle, D.; Schlettwein, D., Fluorinated Phthalocyanines as Molecular Semiconductor Thin Films, *Phys. Status Solidi A* **2008**, *205*, 409-420.

47. Meiss, J.; Merten, A.; Hein, M.; Schuenemann, C.; Schäfer, S.; Tietze, M.; Urich, C.; Pfeiffer, M.; Leo, K.; Riede, M., Fluorinated Zinc Phthalocyanine as Donor for Efficient Vacuum-Deposited Organic Solar Cells, *Adv. Funct. Mater.* **2012**, *22*, 405-414.
48. Mayer, T.; Hunger, R.; Klein, A.; Jaegermann, W., Engineering the Line up of Electronic Energy Levels at Inorganic–Organic Semiconductor Interfaces by Variation of Surface Termination and by Substitution, *Phys. Status Solidi B* **2008**, *245*, 1838-1848.
49. Kam, K. K.; Parkinson, B. A., Detailed Photocurrent Spectroscopy of the Semiconducting Group VIB Transition Metal Dichalcogenides, *J. Phys. Chem.* **1982**, *86*, 463-467.
50. Coy Diaz, H.; Addou, R.; Batzill, M., Interface Properties of CVD Grown Graphene Transferred onto MoS₂(0001), *Nanoscale* **2014**, *6*, 1071-1078.
51. Böker, T.; Severin, R.; Müller, A.; Janowitz, C.; Manzke, R.; Voß, D.; Krüger, P.; Mazur, A.; Pollmann, J., Band Structure of MoS₂, MoSe₂, and α -MoTe₂: Angle-Resolved Photoelectron Spectroscopy and Ab Initio Calculations, *Phys. Rev. B: Condens. Matter* **2001**, *64*, 235305.
52. Fahlman, M.; Sehati, P.; Osikowicz, W.; Braun, S.; de Jong, M. P.; Brocks, G., Photoelectron Spectroscopy and Modeling of Interface Properties Related to Organic Photovoltaic Cells, *J. Electron. Spectrosc. Relat. Phenom.* **2013**, *190*, 33-41.
53. Bao, Q. Y.; Liu, X. J.; Braun, S.; Gao, F.; Fahlman, M., Energetics at Doped Conjugated Polymer/Electrode Interfaces, *Adv. Mater. Interfaces* **2015**, *2*, 1400403.
54. Ishii, H.; Sugiyama, K.; Ito, E.; Seki, K., Energy Level Alignment and Interfacial Electronic Structures at Organic/Metal and Organic/Organic Interfaces, *Adv. Mater.* **1999**, *11*, 605-625.
55. Peisert, H.; Knupfer, M.; Fink, J., Energy Level Alignment at Organic/Metal Interfaces: Dipole and Ionization Potential, *Appl Phys Lett* **2002**, *81*, 2400-2402.
56. Koch, N., Energy Levels at Interfaces between Metals and Conjugated Organic Molecules, *J. Phys.-Condes. Matter* **2008**, *20*, 12.
57. Khoshkhoo, M. S.; Peisert, H.; Chasse, T.; Scheele, M., The Role of the Density of Interface States in Interfacial Energy Level Alignment of PTCDA, *Org. Electron.* **2017**, *49*, 249-254.
58. Knupfer, M.; Peisert, H., Electronic Properties of Interfaces between Model Organic Semiconductors and Metals, *Phys. Status Solidi A* **2004**, *201*, 1055-1074.
59. Koch, N., Organic Electronic Devices and Their Functional Interfaces, *ChemPhysChem* **2007**, *8*, 1438-1455.
60. Duhm, S.; Heimel, G.; Salzmann, I.; Glowatzki, H.; Johnson, R. L.; Vollmer, A.; Rabe, J. P.; Koch, N., Orientation-Dependent Ionization Energies and Interface Dipoles in Ordered Molecular Assemblies, *Nat. Mater.* **2008**, *7*, 326-332.
61. Vazquez, H.; Dappe, Y. J.; Ortega, J.; Flores, F., Energy Level Alignment at Metal/Organic Semiconductor Interfaces: "Pillow" Effect, Induced Density of Interface States, and Charge Neutrality Level, *J. Chem. Phys.* **2007**, *126*.
62. Yamane, H.; Yoshimura, D.; Kawabe, E.; Sumii, R.; Kanai, K.; Ouchi, Y.; Ueno, N.; Seki, K., Electronic Structure at Highly Ordered Organic/Metal Interfaces: Pentacene on Cu(110), *Phys. Rev. B: Condens. Matter* **2007**, *76*, 165436.
63. Betti, M. G.; Kanjilal, A.; Mariani, C.; Vázquez, H.; Dappe, Y. J.; Ortega, J.; Flores, F., Barrier Formation at Organic Interfaces in a Cu(100)-Benzenethiolate-Pentacene Heterostructure, *Phys. Rev. Lett.* **2008**, *100*, 027601.
64. Oehzelt, M.; Koch, N.; Heimel, G., Organic Semiconductor Density of States Controls the Energy Level Alignment at Electrode Interfaces, *Nat. Commun.* **2014**, *5*, 4174.
65. Chassé, T.; Wu, C. I.; Hill, I. G.; Kahn, A., Band Alignment at Organic-Inorganic Semiconductor Interfaces: Alpha-NPD and CuPc on InP(110), *J. Appl. Phys.* **1999**, *85*, 6589-6592.
66. Ueno, N.; Kera, S., Electron Spectroscopy of Functional Organic Thin Films: Deep Insights into Valence Electronic Structure in Relation to Charge Transport Property, *Prog. Surf. Sci.* **2008**, *83*, 490-557.

67. Ueno, N.; Kera, S.; Sakamoto, K.; Okudaira, K. K., Energy Band and Electron-Vibration Coupling in Organic Thin Films: Photoelectron Spectroscopy as a Powerful Tool for Studying the Charge Transport, *Appl. Phys. A* **2008**, *92*, 495-504.
68. de Jong, M. P.; Friedlein, R.; Sorensen, S. L.; Öhrwall, G.; Osikowicz, W.; Tengsted, C.; Jönsson, S. K. M.; Fahlman, M.; Salaneck, W. R., Orbital-Specific Dynamic Charge Transfer from Fe(II)-Tetraphenylporphyrin Molecules to Molybdenum Disulfide Substrates, *Phys. Rev. B: Condens. Matter* **2005**, *72*, 035448.
69. Racke, D. A.; Monti, O. L. A., Persistent Non-Equilibrium Interface Dipoles at Quasi-2D Organic/Inorganic Semiconductor Interfaces: The Effect of Gap States, *Surf. Sci.* **2014**, *630*, 136-143.
70. Racke, D. A.; Kelly, L. L.; Monti, O. L. A., The Importance of Gap States for Energy Level Alignment at Hybrid Interfaces, *J. Electron. Spectrosc. Relat. Phenom.* **2015**, *204*, 132-139.
71. Mahatha, S. K.; Patel, K. D.; Menon, K. S. R., Electronic Structure Investigation of MoS₂ and MoSe₂ Using Angle-Resolved Photoemission Spectroscopy and Ab Initio Band Structure Studies, *J. Phys.: Condens. Matter* **2012**, *24*, 475504.
72. Mattheiss, L. F., Band Structures of Transition-Metal-Dichalcogenide Layer Compounds, *Physical Review B* **1973**, *8*, 3719-3740.
73. Fuhr, J. D.; Sofo, J. O.; Saúl, A., Adsorption of Pd on MoS₂(1000): Ab Initio Electronic-Structure Calculations, *Phys. Rev. B: Condens. Matter* **1999**, *60*, 8343-8347.
74. Offenbacher, H.; Lüftner, D.; Ules, T.; Reinisch, E. M.; Koller, G.; Puschnig, P.; Ramsey, M. G., Orbital Tomography: Molecular Band Maps, Momentum Maps and the Imaging of Real Space Orbitals of Adsorbed Molecules, *J. Electron. Spectrosc. Relat. Phenom.* **2015**, *204*, Part A, 92-101.
75. Grüninger, P.; Greulich, K.; Karstens, R.; Belsler, A.; Ovsyannikov, R.; Giangrisostomi, E.; Bettinger, H. F.; Batchelor, D.; Peisert, H.; Chasse, T., Highly Oriented Hexacene Molecules Grown in Thin Films on Cu(110)-(2 X 1)O, *J. Phys. Chem. C* **2019**, *123*, 27672-27680.
76. Shang, M.-H.; Nagaosa, M.; Nagamatsu, S.-i.; Hosoumi, S.; Kera, S.; Fujikawa, T.; Ueno, N., Photoemission from Valence Bands of Transition Metal-Phthalocyanines, *J. Electron. Spectrosc. Relat. Phenom.* **2011**, *184*, 261-264.
77. Wießner, M.; Zirotti, J.; Forster, F.; Arita, M.; Shimada, K.; Puschnig, P.; Schöll, A.; Reinert, F., Substrate-Mediated Band-Dispersion of Adsorbate Molecular States, *Nat. Commun.* **2013**, *4*, 1514.

TOC Graphic

